Journal of Materials and Environmental Sciences
ISSN : 2028-2508
CODEN : JMESCN

J. Mater. Environ. Sci., 2018, Volume 9, Issue 3, Page 783-793

https://doi.org/10.26872/jmes.2018.9.3.86

http://www.jmaterenvironsci.com

Numerical modeling of the thermal behavior of a direct solar dryer with auxiliary heating system

H. Samrani[1*], A. Ourhedja[1], M.N. Bargach[1], R. Tadili[1], K. Kabidi[3], A. Mcheqrane[2]

1.Department of Physics, Laboratory of Solar Energy and Environment, Faculty of Sciences, Mohammed V University, B.P. 1014, Rabat, Morocco.
2.Department of Electrical Engineering, Laboratory of Renewable Energies and Intelligent Systems Sciences and technologies Faculty, Sidi Mohamed Ben AbdellahUniversity, Fez-Morocco.
3.Direction Régionale de la Météorologie du Nord-Ouest, Direction de la Météorologie Nationale.

Received 13 Jul 2017,
Revised 15 Sep 2017,
Accepted 17 Sep 2017

Keywords
- ✓ Direct solar dryer,
- ✓ Solar radiation,
- ✓ Solar transmittance
- ✓ Temperatures,
- ✓ heating systems,

H Samrani
hamidsamrani@yahoo.fr
+212661658150

Abstract
In this study, we present thermal results related to the heating effect on the microclimate of a direct solar dryer (DSD). The heating effect is tested under two types of climatically different days: aclear day and a cloudy day. A comparison of the results of the numerical simulation and the experimental tests showed a good agreement and covered two types of heating systems: one radiative and the other convective. Their performance, which depends at the same time on the ambient climatic conditions and the thermal performance of the dryer, is decisive as to the advantage and the disadvantage of each and their appropriation to maintain an appropriate setpoint temperature.

1. Introduction
The spontaneous establishment of a microclimate inside a direct solar dryer (DSD) is a direct consequence of the interactions between the components of the dryer (roofing, inside air, soil, etc.) and variables characterizing climatic conditions (solar radiation, ambient temperature, wind speed, etc.). During a day, the thermal behavior of the dryer is different between day and night. Good sealing of the dryer and low transmittance of the cover to infrared radiation are in demand during the night, because they allow a reduction of energy losses. While satisfactory transmission of solar radiation inside the dryer and adequate ventilation are required during the day, it is necessary to increase the greenhouse effect and to promote the evacuation of moist air.
During winter, the weather conditions are such that during the night, temperatures can reach low values causing a significant drop in temperatures inside the dryer. In order to maintain an acceptable set temperature, in relation to the product to be dried, the period and the dryer implantation site, heating is then necessary although its use generates heavy loads due to the increase in the energy cost and occasions the installation of infrastructures that are difficult to handle.
In this study, it is proposed to determine the thermal performance of a (DSD) using a theoretical model for the numerical simulation of its thermal behavior. This model is based on the classical heat transfer equations between the different components of the system and the external environment. The simulation results are compared with the experimental ones.

2. Experimental details
2.1. Site of the installation
The experimental installation is located at the Faculty of Sciences of Rabat. Located on the west coast of Morocco, at 65 m altitude, the climate of the site of Rabat is of the Mediterranean type with a rainy and cold winter and a hot and humid summer. The ambient temperature is moderate throughout the year and represents a small daily amplitude, with an annual average close to 18.4 °C. The average seasonal temperatures are 23.1 °C in summer, 17.8 ° in autumn, 14.9 °C in winter and 18.7 °C in spring. The minimum average is close to 9.9 °C

and maximum is close to 26.2 °C. The annual solar radiation is about 1900 kWh/m^2 with an average insolation time of about 2770 hours per year [1].

2.2. Solar dryer

The different solar fluxes intercepted by the dryer cover (consisting of five facades) are calculated for a prototype solar dryer of standard geometry [2-8]. Four facades are made of transparent glass with a thickness of 6 mm, and the fifth one (wall facing north) of opaque plastic. A perspective view of the used dryer is shown schematically in Figure 1, below.

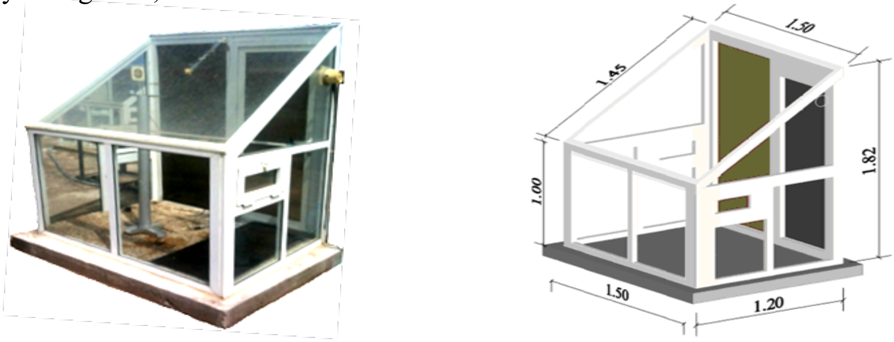

Figure 1: Perspective view of the prototype of a standard dimension

2.3. Measured variables

The Measured variables concern the climatic ones that characterize the external environment and the inner microclimate of the dryer. Using a CR10X data acquisition system with AM25T extension, measurementsare collected every 15 minutes, and then stored in a computer file. Particular attention was accorded to the calibration of the various sensors and measuring instruments. Systematic controls and permanent verifications of the measurements were carried out.

2.3.1. Climate variables

The external ambient temperature and relative humidity are measured using K-type thermocouples and J & R hydroelectric instruments, respectively. The speed and the directionof windare measured at a level of 10 m from the ground. The global horizontal radiation is measured by means of two calibrated Eppleypyranometers, placed above and under the glazed cover, respectively.

2.3.2. DSDoperating temperatures

In addition to the climatic variables measured outside the dryer, its thermal performances are determined from its operating temperatures that relate to the temperature and relative humidity of inside air, glazing and floor temperatures. The measurement of the global radiation transmitted inside the dryer makes it possible to determine the transmission coefficient of the glazing of the cover.

2.4. Mathematical formulation

2.4.1. Limit conditions

The solar dryer is a physical system composed of nine elements: the cover (c)(five elements), the inside air (ai), the inside air vapor mass (Wai), the upper surface layer of the soil (So) and the lower soil layer (S). Nine energy balance equations are therefore needed to describe the system. Each equation is written in terms of the exchange of thermal powers. The explanation and determination of each term are given in Annex A. To define the conditions at the limits of the dryer, the following climatic variables will be considered constant during each simulation step: global solar radiation (Sg), ambient air temperature T_{ae} and relative humidity (HRe), Wind speed (Ue) and deep soil temperature (T_{sp}). The initial conditions at time t = 0 are:

$$T_{v1}(t=0) = T_{v2}(t=0) = T_{v3}(t=0) = T_{v4}(t=0) = T_{pl}(t=0) = T_{ae}(t=0);$$
$$T_{ai}(t=0) = T_{ae}(t=0);$$
$$T_{so}(t=0) = (T_{ai} + T_{sp})/2\ ;$$
$$T_{s}(t=0) = T_{so}\ ;$$
$$W_{ai}(t=0) = W_{ae}(t=0).$$

Temperatures T_{vi} correspond to the different faces of the glazed cover of the dryer. The plastic wall is characterized by its T_{pl} temperature.

2.4.2. Equations of thermal balances

Figure 2 schematizes the set of heat flows exchanged per unit of exchange surface area, between the dryer and its environment:

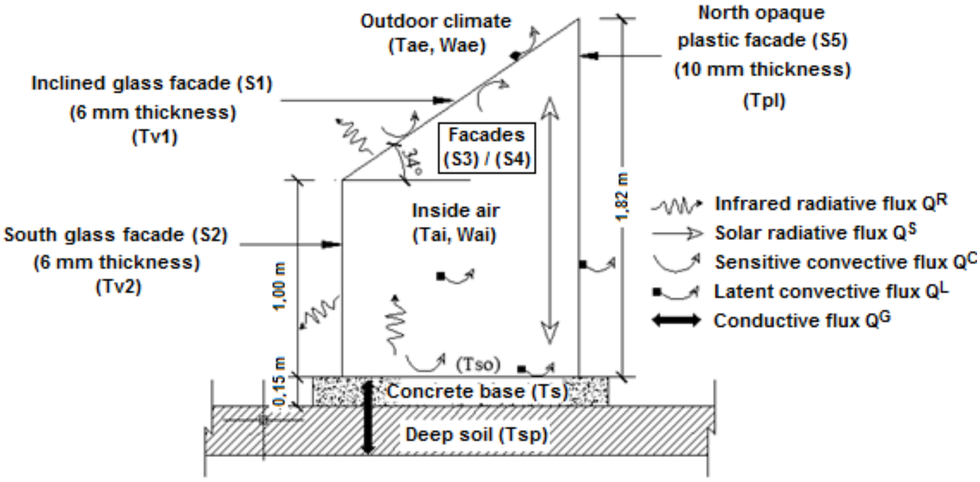

Figure 2: Schematic of exchanged flows

By applying the principle of energy conservation for each element of the dryer, the balance equations are expressed using these thermal fluxes according to the relationship [9-15]:

Σ Contributions - Σ Losses = Variation of internal energy.

For each element i of the dryer:

- the absorbed solar powers will be designated by Q_i^S, respectively;
- the infrared radiative powers exchanged between elements' and j ≠i, as well as the external environment (outside ground, outside air, celestial vault) will be designated by $Q^R_{i,j\neq i}$;
- the sensible convective powers exchanged between the dryer element i and the indoor or outdoor air will be designated by $Q^C_{i,\,air}$;
- the latent convective powers exchanged between the element i of the dryer and the indoor or outdoor air will be designated by $Q^L_{i,\,air}$;
- the power exchanged by conduction at the soil layers So, S and Sp will be designated by $Q^G_{S,\,Si}$.

The expressions of the different heat flux powers involved in the balance equations (relations 1 to 9) as well as the different coefficients of exchange and the choice criteria of the convective modes of exchange (laminar or turbulent regimes, natural or forced convection mode) will be given in Annex A.

2.4.2.1. Thermal balance of coverage

The cover is composed of five surfaces S_i of which four are transparent glass of 6mm thickness, and the fifth is opaque plastic insulated 10mm thick. Each wall $S_i$will be characterized by its temperature T_{vi} (the index i denotes the different glazed faces of the dryer). The plastic wall, facing north, is characterized by its T_{pl} temperature.

The geometric and physical characteristics of the five walls of the cover and soil are given in Table 1 of Appendix B. The balance equations of surfaces S_i of the cover are expressed using relations (1) to (5):

- *Surface S_1 :*

$$Q^S_{v1} - Q^R_{v1,v2} - Q^R_{v1,v3} - Q^R_{v1,v4} - Q^R_{v1,pl} - Q^R_{v1,so} - Q^R_{v1,c} - Q^R_{v1,se} - Q^C_{v1,ai} - Q^C_{v1,ae} - Q^L_{v1,ai} - Q^L_{v1,ae} = \rho_v.c_{v1}.V_{v1}.\frac{dT_{v1}}{dt} \quad (1)$$

- *Surface S2 :*

$$Q^S_{v2} - Q^R_{v2,v1} - Q^R_{v2,v3} - Q^R_{v2,v4} - Q^R_{v2,pl} - Q^R_{v2,so} - Q^R_{v2,c} - Q^R_{v2,se} - Q^C_{v2,ai} - Q^C_{v2,ae} - Q^L_{v2,ai} - Q^L_{v2,ae} = \rho_v.c_{v2}.V_{v2}.\frac{dT_{v2}}{dt} \quad (2)$$

- *Surface S3 :*

$$Q^S_{v3} - Q^R_{v3,v1} - Q^R_{v3,v2} - Q^R_{v3,v4} - Q^R_{v3,pl} - Q^R_{v3,so} - Q^R_{v3,c} - Q^R_{v3,se} - Q^C_{v3,ai} - Q^C_{v3,ae} - Q^L_{v3,ai} - Q^L_{v3,ae} = \rho_v.c_{v3}.V_{v3}.\frac{dT_{v3}}{dt} \quad (3)$$

- *Surface S4 :*

$$Q^S_{v4} - Q^R_{v4,v1} - Q^R_{v4,v2} - Q^R_{v4,v3} - Q^R_{v4,pl} - Q^R_{v4,so} - Q^R_{v4,c} - Q^R_{v4,se} - Q^C_{v4,ai} - Q^C_{v4,ae} - Q^L_{v4,ai} - Q^L_{v4,ae} = \rho_v . c_{v4} . V_{v4} . \frac{dT_{v4}}{dt} \quad (4)$$

- *Surface S5 :*

$$Q^S_{pl} - Q^R_{pl,v1} - Q^R_{pl,v2} - Q^R_{pl,v3} - Q^R_{pl,v4} - Q^R_{pl,so} - Q^R_{pl,c} - Q^R_{pl,se} - Q^C_{pl,ai} - Q^C_{pl,ae} - Q^L_{pl,ai} - Q^L_{pl,ae} = \rho_{pl} . c_{pl} . V_{pl} . \frac{dT_{pl}}{dt} \quad (5)$$

2.4.2.2. Thermal balance of soil

The soil is composed of two superimposed layers, the upper layer (S_o) is in direct contact with the inside air of the dryer, and the lower layer (S) is in direct contact with the deep soil (S_p).

- *Thermal balance of the soil surface layer So*

The thermal balance of the upper layer (So) of the soil can be written as:

$$Q^S_{so} - Q^R_{so,v1} - Q^R_{so,v2} - Q^R_{so,v3} - Q^R_{so,v4} - Q^R_{so,pl} - Q^R_{so,c} - Q^R_{so,se} - Q^C_{so,ai} - Q^C_{so,ae} - Q^L_{so,ai} - Q^L_{so,ae} - Q^G_{so,s} = \rho_s . c_s . V_{so} . \frac{dT_{so}}{dt} \quad (6)$$

- *Thermal balance of the lower soil layer S*

The thermal balance of the lower soil layer is:

$$Q^G_{so,s} - Q^G_{s,sp} = \rho_s . c_s . V_s . \frac{dT_s}{dt} \quad (7)$$

In this equation, the power exchanged by conduction between the lower soil layer S and the deep soil Sp depends on the temperatures Ts and Tsp.With increasing depth, warming or cooling of the soil caused by changes in temperature between day and night is achieved with a time lag and a decrease in amplitude.For a given depth z,we consider in a first approximation that the temperature $T_{Sp}$of the deep soil remains constant.

2.4.2.3. Thermal balance of indoor air

The equation governing the thermal balance of indoor air is written from the thermal powers exchanged by sensible convection between the indoor air and the other elements of the dryer:

$$- Q^C_{ai,v1} - Q^C_{ai,v2} - Q^C_{ai,v3} - Q^C_{ai,v4} - Q^C_{ai,pl} - Q^C_{ai,so} - Q^C_{ai,ae} + QX = \rho_{ai} . c_{ai} . V_{ai} . \frac{dT_{ai}}{dt} \quad (8)$$

c_{ai} is the specific heat of air ($J.kg^{-1}.K^{-1}$)

$Q^C_{ai,ae}$ is the thermal power exchanged between the inside air and the outside air of the dryer by natural renewal through the structure of the dryer.

QX is the supply of heating power of inside air which will be considered zero in the absence of heating.

2.4.2.4. Water Balance of insideair

The equation governing the water balance of the inside air is based on the thermal powers exchanged by latent convection between the inside air and the other dryer elements:

$$- Q^L_{ai,v1} - Q^L_{ai,v2} - Q^L_{ai,v3} - Q^L_{ai,v4} - Q^L_{ai,pl} - Q^L_{ai,so} - Q^L_{ai,ae} = \rho_{ai} . c_{Lai} . V_{ai} . \frac{dW_{ai}}{dt} \quad (9)$$

C_{Lai} is the specific latent heat of water vaporization ($J.kg^{-1}.K^{-1}$).

$Q^L_{ai,ae}$ is the latent heat power exchanged by natural renewal between the indoor air and the outside air, through the dryer structure.

2.4.3. Digital resolution method

Equations (1) to (9) form a system of first-order differential equations of the type:

$$\frac{dYi}{dt} = (Y_i)' = f_i \left[t, Y_1(t), Y_2(t), ..., Y_n(t)\right] \quad (10)$$

Among the many algorithms used to solve this type of equation system, the Runge-Kutta method of order 4 was chosen. It is based on a limited development of the functions, Yi defined as follows:

$$Yi(t_o + \Delta t) = Y_i(t_o) + Y_i'(t_o) . \Delta t + Y_i''(t_o) . \frac{\Delta t^2}{2!} + ... + Y_i^n(t_o) . \frac{\Delta t^n}{n!} \quad (11)$$

The method makes it possible to calculate the coordinates of the following point (t_1, Y_1), then (t_2, Y_2) and so on, with $t_1 = t_o + \Delta t$, $t_2 = t_1 + \Delta t$, ...,$t_n = t_{n-1} + \Delta t$, where Δt represents the time step.

In the system of equations (1) to (9), the initial conditions corresponding to the temperatures measured at the time $t_o$are indicated previously (see § 4.1):
These boundary conditions are imposed by the characteristics of the solar dryer. The inputs of the simulation program correspond to the climatic parameters Sg, Tae, HRe, Ueand Tsp which are regularly measured every 15 minutes.
The following assumptions were considered:

- heat transfers are assumed to be unidirectional;
- the temperatures of each element of the dryer are assumed to be uniformly distributed;
- during a simulation step, the ambient temperature Tae, the global solar radiation Sg and the wind speed Ue are assumed to remain constant or vary slightly;
- the constructive and operational parameters of the solar dryer (covering, soil, indoor air, etc.) are not explicit functions of time, they are always implicit functions of their temperature;
- the temperature of the surrounding soil surface T_{se} is assumed to be equal to that of the ambient temperature Tae, and the apparent temperature of the sky T_c is calculated by the relation:

$$T_c = T_{sn} \times \frac{N}{8} + T_{sc} \times \left(1 - \frac{N}{8}\right)$$

Where Tsnis the temperature of a covered sky, estimated from Arinze's relation [16]:

$$T_{sn} = T_{ae} - 6 \qquad (T_{sn} \text{ and } T_{ae} \text{ in Kelvin}),$$

and$T_{sc}$is the temperature of a clear sky, estimated from the relationship of Swinbank [17]:

$$T_{sc} = 0{,}05532 \times (T_{ae} + 273{,}15)^{1{,}5} \qquad (T_{sc} \text{ and } T_{ae} \text{ in Kelvin}).$$

N is the coefficient of cloudiness that varies between N = 0 for a very clear sky, and N = 8 for a completely covered sky.

3. Results and Discussions

In order to evaluate the temperatures of the different elements of the dryer, the model described above takes into account the meteorological data collected during one year (2013). Only two climatically different days (a clear summer day and a covered winter day) were chosen for validation of the model.

3.1. Validation of the model

Among the temperatures estimated by the model, the temperature of the inside air of the dryer is the most important because its variation directly affects the temperatures of the other elements. As a result, its knowledge is of major interest in determining the performance of the dryer, whatever the climatic conditions prevail, and without the need to resort to measurements. The following figures 3(a) and 3(b) represent the variation profiles of the measured temperature Tai (in bold lines) and the calculated one (in normal lines) during the two studied days (January 15, 2013 for the winter day, and August 15, 2013 for the summer day), respectively:
The comparison of variation profiles of the measured and calculated temperature T_{ai} shows a satisfactory agreement. For the two days studied, the estimation error does not exceed 1.5 °C in the middle of the day and increases slightly at the beginning and the end of the day, due to the relatively high inertia of the air inside the dryer, which slightly delays the response of the dryer to the rapid variation in ambient climate parameters.

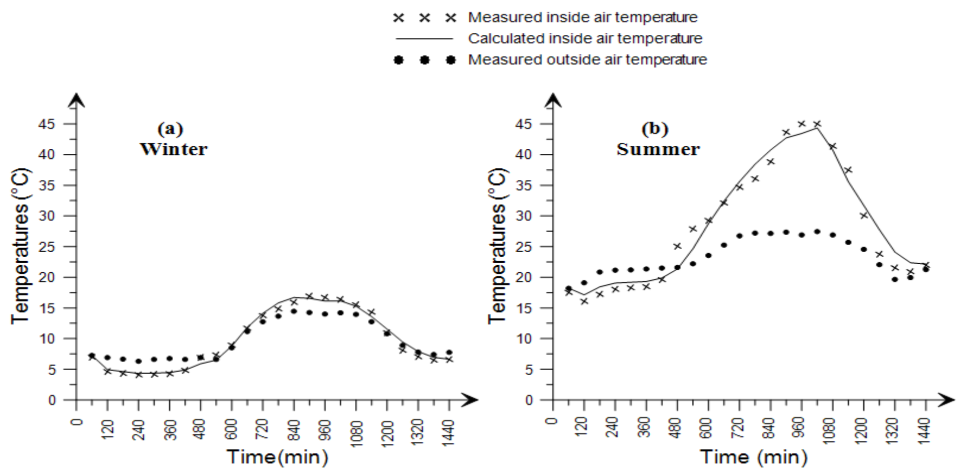

Figure 3: Measured and calculated variations of the inside air temperature of the solar dryer

These profiles show that the amplitude of variation of the temperature Tai inside the dryer between day and night is higher in summer was around 30 °C (between maximum and minimum), compared with onlyto 10 °C in the winter. The offset from midday of recorded maxima is more than four hours in summer, comparedto about three hours in winter.
Due to the IR thermal losses, which are important in winter as well as in summer, it is observed that:
- in the night period, the temperature $T_{ai}$is reversed and becomes lower by approximately 3 to 4 °C than the ambient outside temperature T_{ae}, the deployment of a thermal screen may prove useful and will make it possible to reduce, or even prevent this inversion of temperature;
- during the day, the temperature difference between the inside and the outside is much higher in summer (around 30 °C) than in winter (8 °C). It is therefore necessary to use heating, especially during the night, because it would keep a higher temperature.

3.2 Quantification of heating power

3.2.1 Heating systems

Heating is an important cost in the operating budget of a dryer, and then the choice of heating mode and the most economical system is necessary. Among the multitude of auxiliary heating used systems, especially in winter (gas boiler, heat pump, oil heating, electric heating, pellet stove and wood insert, etc.), the minimum power to be used is dependent on the surrounding climatic conditions and the volume of the air to be heated.
In order to validate the response of our model to the use of a heating system, we tested two heating systems, one of which is radiative, and the other is convective.

3.2.1.1. Radiant heating system

The tested radiative system consists of an electric heating plate with a radiating surface of 700 cm^2, inserted inside the dryer.The choice of the radiating surface of 700 cm² is conditionedby the standard dimensions of the commercially available heating plates. Even the choice of a larger area (equal to the surface of the dryer for example) remains insufficient to ensure the desired setpoint temperature.The heating plate with nominal temperature T_{ch} = 160 °C and the elements of the dryer, in particular the cover whose mean temperature T_m is much less than T_{ch}, are considered to act as gray bodies radiating one to the other, with emissivity ε_1 and ε_2, respectively.
The power radiated by the surface A_1 of the heating plate, to the surface A_2 of the dryer cover, is given by the equation [18]:

$$Q_{12}^{R} = \frac{\sigma.\varepsilon_1.\varepsilon_2.A_1.F_{12}}{1 - (1 - \varepsilon_1).(1 - \varepsilon_2).F_{12}.F_{21}} \left(T_{ch}^4 - T_m^4\right)$$

Where F_{12} and F_{21} are the respective shape factors between the surfaces A_1 and A_2, and σ the Stefan-Boltzmann constant.
Since the product, $(1-\varepsilon_1).(1-\varepsilon_2).F_{12}.F_{21}$ is much less than 1, this equation can be simplified and becomes:

$$Q_{12}^{R} = \sigma.\varepsilon_1.\varepsilon_2.A_1.F_{12} \left(T_{ch}^4 - T_m^4\right)$$

Since the surface A_1 of the heating plate is very small with regard to surface A_2, the shape factors will be $F_{12} \approx 1$ and $F_{21} \approx 0$. Furthermore, considering that the radiating surfaces are black bodies, the emissivity's$\varepsilon_1$and ε_2 are equal to 1, and the power radiated by the heating plate is reduced to the expression:

$$Q_{12}^{R} = A_1.h_{12} \,.\, \left(T_{ch}^4 - T_m^4\right)$$

where the radiative coefficient h_{12} is given by the relation:

$$h_{12} = \sigma \,.\, \left(T_{ch} + T_m\right) . \left(T_{ch}^2 + T_m^2\right)$$

For a maximum temperature of the heating plate Tch = 160 °C and a minimum winter average temperature of the cover Tm = 5 °C, the radiative coefficient h_{12} is equal to about 10.7 $W.m^{-2}.K^{-1}$. Under these conditions, the nominal power corresponding to the maximum power which would be radiated by the heating plate is:
Qmax = 116 W. This power value remains largely below the minimum value required to maintain a desired set temperature T_{set}during the heating period. Therefore, the use of the heating plate is not suitable for auxiliary heating, since in addition to the high energy consumption, necessary for its supply, the thermal requirements (as indicated by curves 4.a and 4.b below), will never be met, especially when the difference between the set point temperature T_{set} and the cover mean temperature T_m, assumed to be close to the outside temperature T_{ae}, is greater than 2 °C.

3.2.1.2. Aero-convective heating system

The installation outside the dryer of a convective heating system, with modular power, made it possible to ensure a heat exchange by renewing air between the outside environment and the inside air of the dryer. The heat exchange is carried out by means of a double pipe, one of which is used for blowing and the other for recovery.

Its application for model validation took into account the technical characteristics of the system, which vary considerably from one system to another (including nominal power and blowing rate) and which cover a very wide range of available products in commerce.

For a heater convection heating system, the following relation calculates the supplementary heating power: to met

$$QX = D \times \rho \times c \times \Delta\theta$$

where D is the volumetric air flow rate (in $m^3.s^{-1}$), ρ is its density (in $kg.m^{-3}$), c is its specific heat (in $J.kg^{-1}.K^{-1}$), and Δθ is the temperature difference between the inlet and the outlet of the heating system, the value of which can reach 100 °C. In the operating temperature range of the dryer, the density ρ of the air and its specific heat c are assumed to be independent of its temperature.

Depending on the required set point temperature T_{set}, the minimum power required for the dryer is always available by this type of heating system.

For the electric heater we tested, with a power of 9 kW = 7740 kcal/hour, maximum hot air flow rate D = 100 m^3/hour and a deviation Δθ = 60 °C with a diameter of 100 mm supply/exhaust ducts, the heating power QXhas reached 1200 W.

The cost price of the heating system remains a major disadvantage in the overall investment cost, but can be easily damped by means of a correct dimensioning of the heating requirements.

3.2.2. Simulation of the heating system

The introduction of heating power into the dryer is necessary in order to maintain its internal air temperature higher than or at least equal to a set temperature T_{set} according to the specificity and nature of the product to be dried.

From the climate data measured on 15/1/2013 and 15/8/2013, several simulations of the heating power QX (voluntarily introduced as a constant in equation 8) have been realized by successive increases of its value between 0 and Nominal power QN, the value of which is linked to external climatic conditions. The chosen variation pitch is 100 W.

The following figures 4.a and 4.b show the variation profiles of QX as a function of the setpoint temperature for the both studied days:

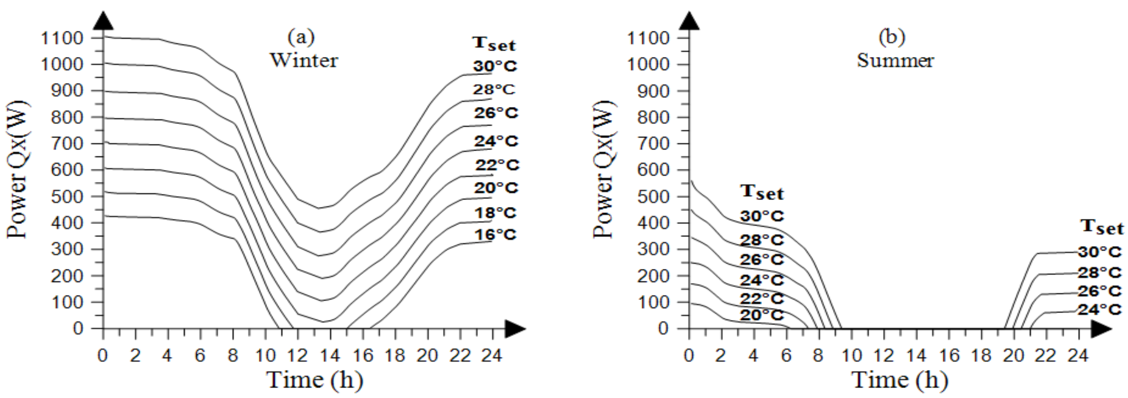

Figure 4: Temporal variations of the heating power QX as a function of the setpoint temperature T_{set}

An analysis of these curves shows that:

- For the winter period, it will be seen that the heating time depends on the set temperature required, which can be reached quickly or not, depending on the ambient climatic conditions. Consequently, the heating time may be longer or shorter, it can even expanded throughout the day for certain temperatures (see figure 5). For the day of 15/01/13, for example, heating is required all day for set temperatures of about 19 °C or more.
- The increase of the set point temperature ΔQX is accompanied by an increase in the heating power. This increase is greater in the nighttime period (ΔQX = 55 W/°C) than in the daytime period (ΔQX = 40 W/°C).

- For the summer period, night heating is only necessary for the highest set temperatures (for a set temperature T_{set} = 30 °C, for example, heating must be provided between 19h PM and 8h AM).
- In the case of lower set temperatures, heating may only occur during the beginning of the day, where the inertia of the air inside the dryer plays a role in maintaining the relatively high internal temperature during the end of day period.
- The curves of figure 4, which show the evolution of the power heating according to the set temperature Tset, are in a range between 16 and 30 °C. Outside this range, heating is not necessary for lower set temperatures (less than 16 °C). For high set temperatures (above 30 °C), many products to be dried are not very resistant to high temperatures, especially during the night.

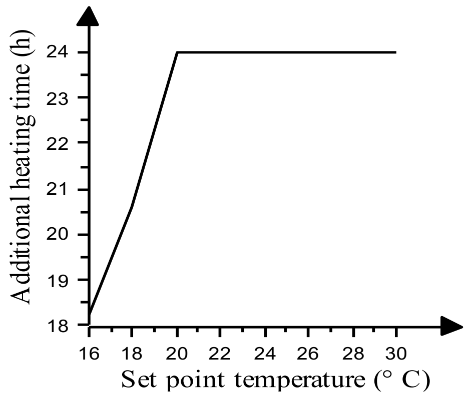

Figure 5: Variation of the heating time as a function of the set temperatures T_{set} in winter.

3.3. Evaluation of heating energy cost

For the assessment of the cost of heating energy, and excluding the initial investment cost, fluctuations and variability in fuel purchase prices, ease of installation of the heating system, necessity of connection to a power source, the need for storage, etc., two scenarios are possible:
- the heating power remains constant during the heating period, the resulting energy is the product of this power by the duration of operation;
- the heating power remains constant over successive short periods and its value changes from one period to another as a function of the desired setpoint temperature, the resulting energy in this case is the sum of the successive energies calculated for each interval.

Based on the estimated heating power variation profile over a day, as a function of the requested set point temperature, the curve (a) in Figure 6 below shows the variation of the daily heating energy calculated for the winter day studied. A quasi-linear increase is obtained as a function of the required temperature of the energy, which vary for a set temperature of 16 °C from 1.5 $kWh.m^{-3}.day^{-1}$, and reaches $8kWh.m^{-3}.day^{-1}$ for an extreme set temperature of 30 °C.

Curve (b) of Figure 6 shows the variation of this daily supplemental heating energy calculated for the summer day studied. It can be seen that this energy, which remains zero for set temperatures below 20 °C., increases slightly for set temperatures above 20 °C., and holds only 1.2 $kWh.m^{-3}.day^{-1}$for the set point extreme temperature of 30 °C.

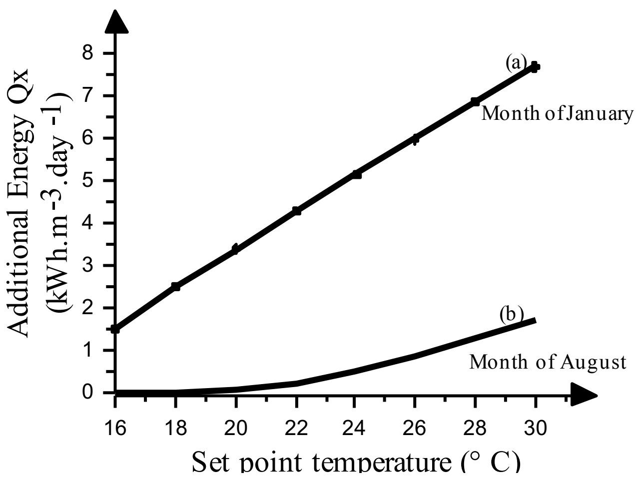

Figure 6: Variations in daily heating energy for both studied days.

Conclusions

The positive comparison between the theoretical model and the experimental results concerned the variation during twoclimatical different days of the air temperature inside the dryer. A maximum deviation of 1.5 °C was observed between the two temperatures (theoretical and experimental).

Deviation between outside and inside temperatures is very high in summer (30 °C) but lower in winter (10 °C).The difference obtained in the winter season is insufficient to initiate the drying process without the need for auxiliary heating.

The results of simulation of the thermal behavior of the dryer as a function of the heating power show that to increase the temperature of the air inside the dryer by 1°C, an auxiliary heating of approximately 55 W overnight against 40 W during the day is necessary in winter. In summer, the need for auxiliary heating is only desired during the night and for very high set point temperatures.

The daily auxiliary heating energy increases linearly depending on the required set point temperature. In winter, the daily heating energy is 1.5 $kWh.m^{-3}.day^{-1}$ for a temperature set point of 16 °C, reaching 8$kWh.m^{-3}.day^{-1}$for an extreme temperature set point of 30 °C.In summer, this energy, which remains zero for set temperatures below 20 °C, increases slightly for set temperatures above 20 °C and requires only 1.2 $kWh.m^{-3}.day^{-1}$for the extreme temperature set point of 30 °C.

NOMENCLATURE

c_{ai}: Mass heat of moist air inside the dryer ($J.kg^{-1}.K^{-1}$).
c_{ae}: Mass heat of moist air outside the dryer ($J.kg^{-1}.K^{-1}$).
c_S: Specific heat of concrete ($J.kg^{-1}.K^{-1}$).
c_v: Specific heat of glass ($J.kg^{-1}.K^{-1}$).
c_{pl}: Specific heat of plexiglas ($J.kg^{-1}.K^{-1}$).
c_{Lai}: Specific latent heat of vaporization of the water($J.kg^{-1}$)
D: Hourly air outflow (Volume/hour).
e: Thickness of upper soil layer S_o(m).
F_{i-j}: Form factor between element i and element j.
Gr: Grashof dimensionless number.
$h_{v,mi}$: Mass transfer coefficient between the Si facade and the inside air ($kg.m^{-2}.s^{-1}$)
$h_{v,me}$: Mass transfer coefficient between the Si facade and the outside air ($kg.m^{-2}.s^{-1}$)
$h_{v,ai}$: Sensitive convective exchange coefficient between the S_i facade and the inside air ($W.m^{-2}.K^{-1}$).
$h_{v,ae}$: Sensitive convective exchange coefficient between the S_i facade and the outside air ($W.m^{-2}.K^{-1}$).
$h_{pl,ai}$: Sensitive convective exchange coefficient between the S_{pl} facade and the inside air ($W.m^{-2}.K^{-1}$).
$h_{pl,ae}$: Sensitive convective exchange coefficient between the S_{pl} facade and the outside air ($W.m^{-2}.K^{-1}$).
$h_{So,ai}$: Sensitive convective exchange coefficient between the upper soil surface S_o and the outside air ($W.m^{-2}.K^{-1}$).
HRe: Relative humidity of outside air (%).
Nu: Nusselt dimensionless number.
Tai: Air temperature inside the dryer (°C).
Tae: Ambient temperature of outside air (°C).
Tc: Apparent temperature of the sky (K).
N: Coefficient of nebulosity.
Pr: Prandtl dimensionless number.
$Q^C_{ai,ae}$ Convective power exchanged between inside air ai and outside air ae (W).
$Q^C_{i,air}$: Sensitive convective power exchanged between the dryer element i and the inside or outside air (W).
$Q^G_{S,Si}$:Power exchanged by conduction between soil layers (W).
$Q^L_{i,air}$: Latent convective power exchanged between the dryer elementi and the inside or outside air (W).
$Q^R_{i,air}$: Infrared radiative power exchanged between element i and elements j ≠i (W).
Q^S_i :Solar power absorbed by element i (W).
QX: Inside air heating power (W).
Re: Reynolds dimensionless number.
So: Surface of the upper soil layer (m^2).
S: Surface of the lower soil layer (m^2).
S_i: Surface of bodyi(m^2).
S1: Surface of the south inclined glass (m^2).
S2 Surface of the south vertical glass (m^2).
S3 Surface of the east vertical glass (m^2).
S4: Surface of the west vertical glass (m^2).
Sg: Global solar radiation ($W.m^{-2}$).
S_{pl} Surface of the north wall (m^2).
St: Surface exchange between solid and inside air (m^2).
T_i: Temperature of body i(K).
T_{pl}: Temperature of the north wall S_{pl} (°C).
Tsc : Temperature of a clear sky (°C).
Ts: Temperature of the lower soil layer (°C).
Tse: Temperature of the outside soil(K).
Tsn: Temperature of a cloudy sky (°C).
T_{so}: Temperature of the upper soil layer (°C).
T_{v1}: Temperature of the south inclined glass S_1 (°C).
T_{v2}: Temperature of the south vertical glass S_2 (°C).
T_{v3}: Temperature of the east vertical glass S_3 (°C).
T_{v4}: Temperature of the west vertical glass S_4 (°C).
Tsp: Deep Soil Temperature (°C).
Ue: Wind speed of the outside air ($m.s^{-1}$).
Vt : Volume of air inside the dryer (m^3).
V_{vi} : Volume of the facade S_i of the dryer (m^3).
V_{pl} : Volume of the facade S_{pl} of the dryer (m^3).
V_S : Volume of the lower soil layer of the dryer (m^3).
V_{So} : Volume of the upper soil layer of the dryer (m^3).
W_{ai}: Inside air vapor mass (kg/kg).
W_{vi} : Saturated humidity at the temperature of facade S_i(kg/kg).
W_{pl} : Saturated humidity at the temperature of facade S_{pl}(kg/kg).
W_{So} : Saturated humidity at the temperature of the upper soil surface S_o(kg/kg).
ε_i Emissivityof bodyi.
λ_{so}: Thermal conductivity of the upper soil surface S_o ($W.m^{-1}.K^{-1}$).
ρ_S: Density of concrete ($kg.m^{-3}$).
ρ_v: Density of glass ($kg.m^{-3}$).
ρ_{pl}: Density of Plexiglas ($kg.m^{-3}$).
ρ_{ai}: Density of the inside air ($kg.m^{-3}$).
σ: Constant of Stefan-Boltzman($W.m^{-2}.K^{-4}$).

ANNEX A

1) Exchanged thermal powers

Power of the convective heat flux exchanged between the facades $S_i$and the outside air (the index i denotes the various glass sides of the dryer):

$$Q^C_{vi,ae}=h_e.S_i.(T_{Vi}-T_{ae})$$

Power of the convective heat flux exchanged between the facades S_i and the inside air:

$$Q^C_{Vi,ai}=h_{Vi,ai}.S_i.(T_{Vi}-T_{ai})$$

Power of the latent convective heat flux exchanged between the facades Si and the outside air:

$$Q^L_{vi.ae}=C_{Lai}.h_{vi.me}.S_i.(W_{vi}-W_{ae})$$

Power of the latent convective heat flux exchanged between the facades Si and the inside air:

$$Q^L_{vi.ai}=C_{L\ ai}.h_{vi.mi}.S_i.(W_{vi}-W_{ai})$$

Convective heat flux due to air leakage:

$$Q^C_{ai.ae}=D.\rho_{ai}.\frac{Vt}{St}.\left(C_{vai}.T_{ai}-C_{vae}.T_{ae}\right)$$

Power exchange by conduction between two successive layers of soil:

$$Q^G_{S.So}=\frac{\lambda_{So}}{e}.S_o.\left(T_S-T_{So}\right)$$

Power of the radiative flux exchanged between surface S_i and surface S_j:

$$Q^R_{vi.vj}=\frac{\sigma.\varepsilon_{vi}.\varepsilon_{vj}.F_{vivj}.S_i}{1-\left(1-\varepsilon_{vi}\right).\left(1-\varepsilon_{vj}\right).F_{vi.vj}.F_{vj.vi}}\left(T^4_{vi}-T^4_{vj}\right)$$

Power of the radiative flux exchanged between the surface S_i and the sky:

$$Q^R_{vi.c}=\sigma.\varepsilon_v.\varepsilon_c.F_{vc}.\left(T^4_v-T^4_c\right)$$

Power of the radiative flux exchanged between the S_i surface and the celestial vault:

$$Q^R_{vi.se}=\sigma.\varepsilon_v.\varepsilon_{se}.F_{vse}.\left(T^4_v-T^4_{se}\right)$$

2) Convective exchange coefficients

The convective coefficient hc,ae (W.m-2.°C^{-1}) between the solar dryer cover and the outside air is assumed to be related only to wind speed Ue (m.s-1) according to McAdam's law [19-20]:

$h_{c,ae}= 7.5 + 3.88\times U_e$ if $U_e<U_{limite}=7.72$ (m.s^{-1}).
$h_{c,ae} = 7.3\times (U_e)^{0.80}$ if $U_e>U_{limite}$.

The convective coefficient $h_{c,ai}$ (W.m^{-2}.°C^{-1}) between the inside air and the solar dryer cover is calculated from the relation:

$$h_{c,ai}=\frac{Nu.\lambda_{ai}}{L_{ci}}$$

The convective coefficient $h_{c,ai}$ (W.m^{-2}.°C^{-1}) between the inside air and the solar dryer cover is calculated from the relation:

$$h_{so,ai}=\frac{Nu\lambda_{ai}}{L_{soil}}$$

λ_{ai} : the thermal conductivity of the air (W.m^{-1}.K^{-1})
L_{ci}: the characteristic length of the coverage considered equal to the ratio between its surface and its perimeter (m).
L_{soil}: the characteristic soil length corresponding to the ratio of the dryer / floor area.

The dimensionless number of Nusselt Nu depends on the nature of the convection (natural or forced) and the mode of flow (laminar or turbulent) [21]:

$$Nu = f\,(Gr, Re)$$

The boundaries between these different modes are defined by the dimensionless numbers of Grashof (Gr), Reynolds (Re) and Prandlt (Pr).

The limit between laminar and turbulent regimes is defined by the product $L_i^3\times\Delta T$.

ANNEX B

Table 1: Geometric and physical parameters of the solar dryer cover

Settings	Materials	surfaces (m^2)	Orientation	Tilt	Density ρ (kg/m^3)	Thermal conductivity λ (W/m.K)	Massic heat C_m (J/kg.K)
Façade (S1) Façade (S2) Façade (S3) Façade (S4)	Glass Of 6mm	2,18 1,5 1,71 1,71	South South East west	34 90 90 90	2500	0,8	840
Façade (S5)	Plexiglas Of 10 mm	2,78	North	90	1170	0,7	1380
Soil (S)	Concrete of 15cm	1,80	-	-	2200	1.8	1000

References

1. J. Bahraoui-Buret J, M.N. Bargach, M.L. Benkaddour, S.M.E.R DIFFUSION(1983).
2. H. Samrani, A. Khyad, M.N. Bargach, R. Tadili, A. Mcheqrane, *IIRE.*10 (2) (2015) 1.
3. K. Kabidi, H. Samrani, M.N. Bargach, R. Tadili, *IIRE.*9 (1) (2014) 1.
4. A. El Khadraoui, S. Bouadila, S. Kooli, A. Farhat, A. Guizani, *J Clean Prod.*,148 (2017) 37.
5. K. Kant, A. Shukla, A. Sharma, A. Kumar, A. Jain, *Innov.Food Sci.Emerg.Technol*. 34(2016) 86.
6. C. Perrin de Brichambaut, G. Lamboley, Cahier AFEDES n°1, Editions Européennes Thermique et Industrie, Paris (1968)
7. J.P. Mathieu, Société d'Édition d'Enseignement Supérieur S.E.D.E.S. Paris (1965).
8. A. Nisen, J. Deltour, J. Nijskins, S. Coutisse, Centre d'Étude des Économies d'Énergie en Cultures Protégées, I.R.S.I.A., Belgique(1986).
9. W.C. McAdams, *McGraw-Hill*, *New York* (1954).
10. D. De Halleux, J. Deltour, J. Nijskins, A. Nisen, S. Coutisse, *Acta Hortic.*170 (1985) 91.
11. D. De Halleux, Thèse de Doctorat es sciences agronomiques, Fac. Sciences Agronomiques, Gembloux, Belgique (1989).
12. J. Deltour, D. De Halleux, J. Nijskins, S. Coutisse, A. Nisen, *Acta Hortic.*174 (1985a) 119.
13. J. Deltour, J. Nijskins, A. Nisen, S. Coutisse, Centre d'Etude des Economies d'Energie en Culture Protégée, R. S.I.A. (1985b).
14. J.A. Duffie, W.A. Beckman, John Wiley and Sons, New York (1980).
15. W.M. Rohsenow, J.P. Hartnett, McGraw-Hill, *New York* (1998).
16. E.A. Arinze, G.J. Schoenau, R.W. Beant, *Trans ASAE.* 27(2*)* (1984) 508.
17. W.C. Swinbank, *Q J Roy Meteorol Soc.*89 (381) (1963) 339.
18. VDI Wärmeatlas, Wärme Atlas, VDI VerlagGmbh, Düsseldorf (1977).
19. C. Monteil, G. Issanchou, M. Amouroux, *J Phys III.*1(3) (1991) 429.
20. F. Meknassi, Thèse de Doctorat 3ème Cycle, Perpignan-France (1983).
21. G. Papadakis, A. Frangoudakis, S. KyritsiMixed, *J Agr Eng Res.*51 (1992) 191.

(2018) ;http://www.jmaterenvironsci.com